Journal of Liquid Chromatography and Gas Chromatography, Europe
https://technicalreport.org/lcgceu/

LC GC Eu., Vol. 38, No.4, 57-64, 2025

Technical Reports Press

RESEARCH ARTICLE

Gate-Linked Readiness Analysis of Piezoelectric Diagnostic Sensors for Near-Patient Analytical Instrumentation

Louis E. Brus[1*]

[2]*Department of Chemistry, Columbia University, New York, New York 10027, USA*
[*]*Corresponding author*

Corresponding author:
leb26@columbia.edu

Abstract
Piezoelectric chemosensors and biosensors translate molecular binding, microbial capture, cellular adhesion, and biomarker recognition into label-free mechanical responses. Their diagnostic value, however, depends on more than a low limit of detection. This study asks which piezoelectric diagnostic sensors satisfy a linked set of near-patient requirements: analyte-relevant signal, explicit sample-to-answer time, transferable resonator format, practical receptor chemistry, medical decision relevance, and sufficient operational documentation. Twelve named sensor architectures were organized as a seventy-two-cell gate matrix using Bottleneck-Resolved Evidence Concordance (BREC), with each architecture evaluated across six readiness gates. The clinical-concordant group consisted of the quartz crystal microbalance aptasensor for K562 cells, the quartz crystal microbalance immunosensor for *Staphylococcus aureus*, and the quartz crystal microbalance procalcitonin biosensor. Heat shock protein and miR-106b sensors showed high analytical strength but were limited respectively by hardware transferability and incomplete sample-to-answer definition. Prostate-specific antigen, lactoferrin, and N^6-methyladenine assays required protocol completion, time compression, or proof that added instrument complexity improves diagnostic discrimination. Molecularly imprinted polymer assays were most coherent as chemical-recognition or toxicology tools rather than bedside medical tests, while the SARS-CoV-2 antibody wafer assay required exact analytical limits and timing before fair comparison. The main conclusion is that piezoelectric diagnostic translation is controlled by the identity of the first unresolved bottleneck, not by detection limit alone.

Keywords: piezoelectric biosensor; quartz crystal microbalance; bottleneck analysis; analytical validation; point-of-care diagnostics; assay documentation; recognition chemistry; diagnostic instrumentation

Received: 10 August 2025
Accepted: 29 November 2025
Available online: 30 December 2025

1. Introduction

Piezoelectric biosensing is attractive for diagnostic instrumentation because a surface recognition event can be converted directly into a mechanical or acoustic signal. In principle, this allows compact readout, label-free operation, and real-time monitoring. In practice, the same physical diversity that makes piezoelectric sensing versatile also complicates evaluation. A bacterial capture assay, a leukemia-cell aptasensor, a nucleic-acid hybridization assay, a protein immunosensor, and a synthetic small-molecule recognition surface do not carry the same diagnostic meaning, even when each is summarized by a numerical detection limit.

The quartz crystal microbalance (QCM) is the most familiar piezoelectric platform because the relationship between rigid surface mass and resonant-frequency change is well established, while liquid-phase operation requires attention to viscosity, density loading, hydration, and interfacial softness [1–4]. These physical constraints are not secondary details in diagnostic work. Serum, plasma, saliva, urine, bacterial suspensions, cell lysates, and food-associated matrices can contribute nonspecific adsorption, unstable fluid loading, or viscoelastic artifacts. A credible diagnostic sensor must therefore connect its frequency response to a controlled sample pathway and a reproducible surface

Cite as: L. E. Brus (2025). Gate-Linked Readiness Analysis of Piezoelectric Diagnostic Sensors for Near-Patient Analytical Instrumentation. LC GC Eu., 38(4) (2025) 57-64.

preparation.

Mechanical and acoustic biosensors have been reviewed as powerful alternatives to optical assays because they can detect binding, mass change, and interfacial events without fluorophores or chromogenic labels [5–10]. Yet the deployment path differs sharply across lateral-field resonators, surface acoustic wave devices, lithium niobate wafers, gold-coated quartz transducers, conventional QCM chips, and hybrid QCM-D/surface-enhanced Raman systems. A specialized resonator may deliver excellent sensitivity, but a near-patient instrument also requires cartridge reproducibility, thermal tolerance, fluidic control, and straightforward calibration.

Recognition chemistry adds another layer of variation. Antibody layers are clinically familiar but must address orientation, immobilization yield, stability, and lot-to-lot variation. Aptamers and hairpin probes can be chemically programmable and traceable to nucleic-acid selection principles [11–13]. Molecularly imprinted polymers offer synthetic recognition surfaces that may be robust and inexpensive, although selectivity must be demonstrated in realistic matrices [14, 15]. Hybrid optical-acoustic detection, including surface-enhanced Raman readout, can increase chemical specificity, but it also adds hardware and interpretation burden that must improve decision quality rather than simply add complexity [16].

Point-of-care diagnostics are judged by clinical actionability, time-to-result, sample handling, robustness, connectivity, operator burden, and cost, not by analytical sensitivity alone [17–22]. Diagnostic validation guidance similarly emphasizes transparent documentation of detection capability, precision, bias, specimen matrix, interference, and accuracy [23–25]. Piezoelectric sensor assessment should therefore ask whether a device has the operational evidence needed for validation: a stated working range, specimen context, total assay time, chip conditioning procedure, receptor immobilization route, replicate structure, and clear interpretation of the readout.

The research question is specific: which piezoelectric diagnostic sensors are concordant across signal, time, platform, receptor, medical-use, and documentation requirements, and which first bottleneck determines the next experiment when concordance is absent? The answer is developed using Bottleneck-Resolved Evidence Concordance (BREC), a gate-based method that preserves the native analytical units of each assay and assigns a readiness lane according to the first condition that blocks near-patient analytical use.

The five-panel overview in Figure 1 defines the measurement domains used throughout the paper. Detectability, specimen context, transducer format, receptor chemistry, documentation quality, and validation direction are treated as connected conditions rather than independent descriptors. This visual logic is important because the later conclusions depend on the relationship among these domains: a sensor with excellent signal can still be limited by unclear timing, unsuitable platform transfer, or insufficient documentation.

The domain overview functions as the organizational map for the analysis. It explains why the study separates target class, platform type, receptor chemistry, assay timing, and documentation rather than merging them into a single sensitivity order. The same limit-of-detection value can have different implications depending on whether the measurement concerns microbial burden, circulating protein, cancer-associated cells, viral antibodies, methylated nucleotides, or small-molecule chemical recognition.

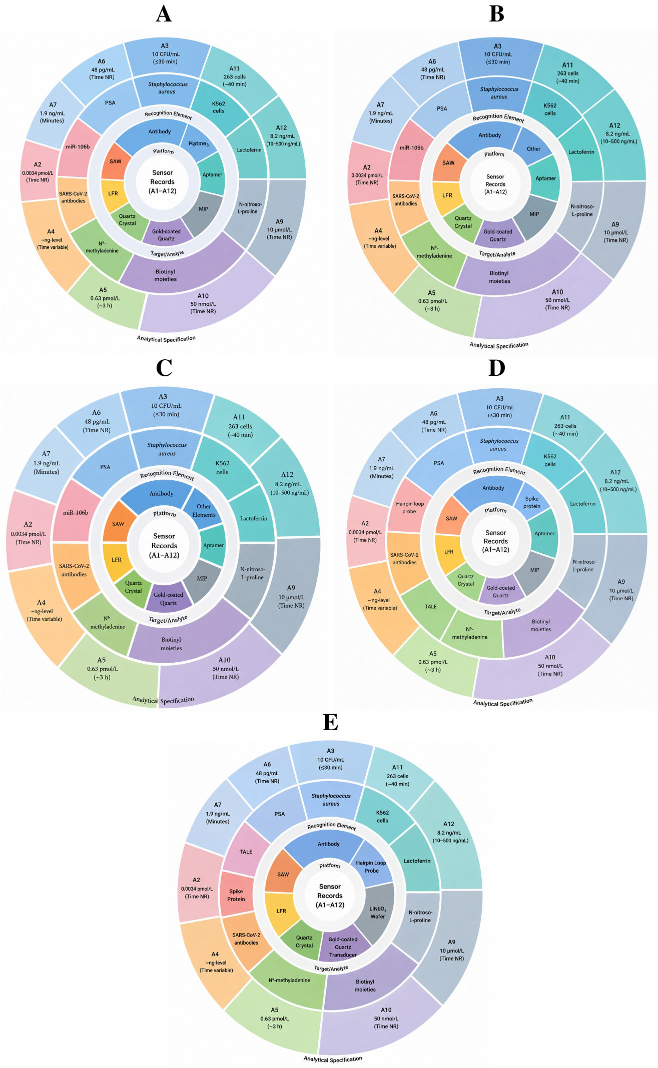

Figure 1: Concordance gate domains.

2. Materials and Methods

2.1. Sensor set and coding principles

Twelve piezoelectric medical-diagnostic sensors were identified from a tabulated survey of chemosensor and biosensor applications [26]. Each sensor was coded by platform, recognition element, target analyte, analytical specification, and time-to-result when numerically available. Native units were retained because pg mL^{-1}, ng L^{-1}, pmol L^{-1}, CFU mL^{-1}, cell count, nmol L^{-1}, and µmol L^{-1} describe different measurement objects and cannot be ranked responsibly on one universal numerical axis.

The structured analytical dataset in Table 1 was used in the BREC analysis. It contains the specific platforms, receptors, analytes, detection limits, ranges, and timing values used for all gate decisions. Missing or approximate entries are retained because absence of timing, range, matrix, or specificity information directly affects readiness for validation.

The dataset contains more than a list of devices; it contains a set of distinct measurement problems. QCM-based formats dominate, but the set also includes lateral-field, surface acoustic wave, lithium niobate, gold-coated quartz, and dual-mode QCM-D/SERS architectures. Recognition elements include antibodies, aptamers, hairpin probes, molecularly imprinted polymers, transcription-activator-like

Table 1: Piezoelectric sensor dataset.

ID	Piezoelectric platform	Recognition element	Target analyte	Analytical specification used for gating
A1	Lateral-field piezoelectric resonator	Antibody	Heat shock proteins from myeloma cells	Limit of detection 7.5 pg mL^{-1}; assay time up to 5 min
A2	$LiTaO_3$ surface acoustic wave substrate	Hairpin loop capture probe	miR-106b from cancer cells	Linear range 0.1 pmol L^{-1} to 1.0 µmol L^{-1}; limit of detection 0.0034 pmol L^{-1}
A3	Quartz crystal microbalance	Antibody	*Staphylococcus aureus*	Limit of detection 10 CFU mL^{-1}; assay time up to 30 min
A4	128° YX lithium niobate piezoelectric wafer	SARS-CoV-2 Spike protein	Antibodies against SARS-CoV-2	Detection from approximately nanogram level; assay duration variable from minutes to hours
A5	Quartz crystal sensor	Transcription-activator-like effectors	N^6-methyladenine	Limit of detection 0.63 pmol L^{-1}; total assay time approximately 3 h
A6	Quartz crystal microbalance	Antibody	Prostate-specific antigen	Limit of detection 48 pg mL^{-1}; assay time not numerically stated
A7	Quartz crystal microbalance with dissipation and surface-enhanced Raman scattering coupling	Nucleic-acid aptamer	Prostate-specific antigen	Limit of detection 1.9 ng mL^{-1}; rapid readout described in minutes
A8	Quartz crystal microbalance	Antibody–gold nanoparticle conjugate	Procalcitonin	Limit of detection 37.8 ng L^{-1}; total assay time less than 1 h
A9	Quartz crystal microbalance	Molecularly imprinted polymer	*N*-nitroso-*l*-proline	Piezoelectric microgravimetry limit of detection 10 µmol L^{-1}
A10	Gold-coated quartz transducer	Molecularly imprinted polymer	Biotin methyl ester and other biotinyl moieties	Limit of detection 50 nmol L^{-1}
A11	Quartz crystal microbalance	Aptamer	K562 cells associated with chronic myeloid leukemia	Limit of detection 263 K562 cells; approximate assay time 40 min per sample
A12	Quartz crystal microbalance	Aptamer	Lactoferrin	Linear detection range 10–500 ng mL^{-1}; limit of detection 8.2 ng mL^{-1}

effectors, and immobilized viral protein. These platform and receptor differences are the reason the analysis assigns readiness lanes rather than a sensitivity-only rank.

The bench-material panels in Figure 2 connect the analytical dataset to the physical operations required in a laboratory assay. Chips, standards, biological media, sample tubes, and frequency-monitoring hardware are not decorative elements; they define whether a frequency shift can be reproduced across operators and instruments. The image therefore supports the methodological decision to treat operational documentation as part of the scientific evidence.

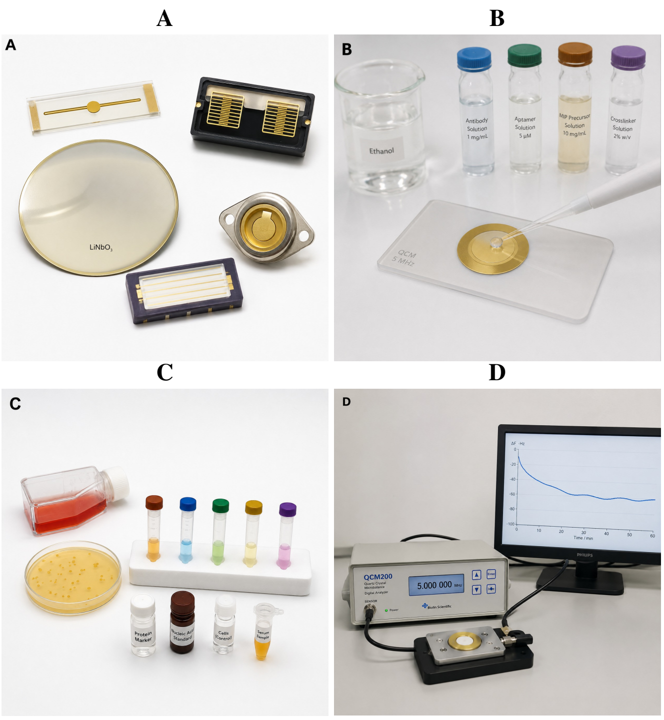

Figure 2: Sensor materials and assay handling.

The material context explains why a limit of detection cannot be interpreted alone. The same numerical sensitivity has different value if it requires unstable chip conditioning, poorly specified washing, undefined sample volume, or a hard-to-transfer resonator. For that reason, the method evaluates assay information as a complete measurement pathway from recognition surface to interpretable readout.

2.2. Bottleneck-Resolved Evidence Concordance method

BREC evaluates each sensor through six gates: signal adequacy, temporal definition, platform transferability, receptor continuity, medical-decision alignment, and documentation sufficiency. A gate is coded as *solid* when the information is explicit and practically meaningful, *conditional* when the information is promising but incomplete or hardware-specific, and *unresolved* when the missing detail would prevent near-patient analytical planning. The outcome is a bottleneck profile rather than a mathematical score.

The six gates in Table 2 define the coding criteria. Signal adequacy is judged within analyte class, not across all numerical units. Temporal definition requires the full assay or sample-to-answer interval. Platform transferability concerns whether the resonator can plausibly move toward a standardized QCM or quartz-cartridge pathway. Receptor continuity covers reproducible fabrication, storage, and surface use. Medical-decision alignment asks whether the target supports infection, cancer, inflammation, sepsis, or hematological decisions. Documentation sufficiency asks whether enough operational detail exists for validation design.

The gate criteria prevent arbitrary weighting. A sensor may have excellent signal adequacy and still remain protocol-limited if sample-to-answer time is missing. Another sensor may use a familiar QCM platform and still remain use-limited if its analyte does not match a bedside medical decision. This structure is useful because it identifies the experiment or documentation item that should be completed next.

The BREC workflow in Figure 3 is organized as a gate ladder. The sequence begins with analyte-relevant signal and medical-decision alignment, proceeds through timing, platform, and receptor checks, and ends with documentation sufficiency and readiness-lane assignment. This order reflects practical development logic: a near-patient sensor must have a meaningful target, credible signal, timed workflow, transferable hardware, reproducible receptor surface, and a validation-ready procedure.

The workflow clarifies why the method does not ask which sensor has the smallest numerical detection limit. It asks where translation would stop first if a laboratory attempted to turn the sensor into a near-patient procedure. The resulting lane assignment can recommend different actions for high-performing sensors, including platform comparison, timed protocol completion, matrix verification, or use-case redirection.

The data-coding audit in Figure 4 illustrates how each assay was read as a combination of target, chip, receptor, sample context, and instrument observation. The visual sequence supports traceability:

Table 2: BREC gate criteria.

Gate	Solid condition	Conditional or unresolved condition
Signal adequacy	Detection or range is strong within the analyte class and stated in usable units.	Approximate, qualitative, weak, or context-poor sensitivity statement.
Temporal definition	Total assay or sample-to-answer time is explicit and compatible with near-patient decision making.	Time is absent, broad, workflow-dependent, or too long for the intended decision.
Platform transferability	Device format is compatible with a plausible standardized QCM or quartz-cartridge pathway.	Hardware is specialized, hybridized, or not yet demonstrated in a deployable format.
Receptor continuity	Recognition element has a plausible route to reproducible preparation, storage, and surface regeneration or single use.	Receptor is biologically complex, difficult to standardize, or insufficiently documented.
Medical-decision alignment	Target is directly linked to infection, cancer, inflammation, sepsis, or hematological monitoring.	Target is mainly chemical, food-toxicological, exploratory, or not yet tied to bedside action.
Documentation sufficiency	Limit, range or specificity context, time, matrix direction, and operational constraints are sufficiently visible for validation planning.	Key elements are missing, approximate, or expressed too broadly for validation planning.

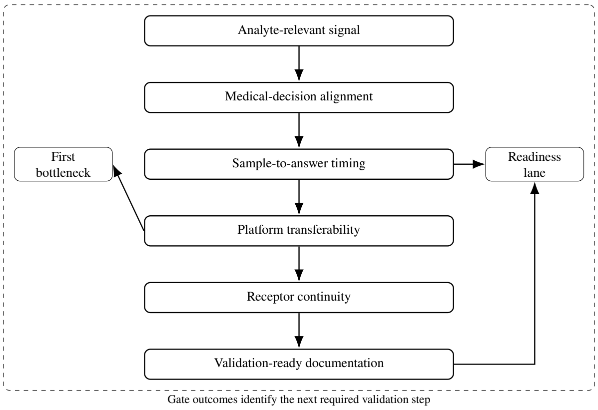

Figure 3: BREC gate workflow.

each readiness claim must be connected to a defined analytical attribute before it becomes a validation recommendation.

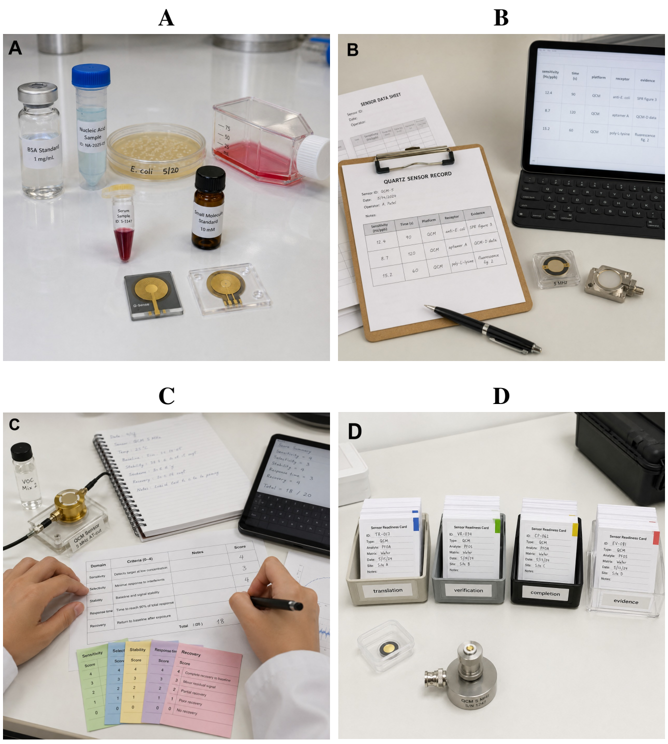

Figure 4: Assay coding audit.

The audit view is important because several lane decisions are driven by absent operational detail rather than by weak analytical performance. Sensors with missing timing, approximate sensitivity statements, or broad procedural descriptions are not rejected; they are assigned to the lane that identifies the exact information needed before stronger diagnostic claims can be made.

3. Results

3.1. Gate-matrix structure

The twelve sensors produced a seventy-two-cell BREC matrix: six gates for each sensor. The matrix is intentionally heterogeneous. Seven sensors used QCM or QCM-derived formats, while the remaining sensors used lateral-field, surface acoustic wave, lithium niobate, gold-coated quartz, or quartz sensor formats. The analytes also differed sharply, including protein biomarkers, microbial cells, cancer-associated cells, nucleic-acid targets, viral antibodies, small molecules, and chemical-recognition targets.

This heterogeneity is the first major result. A table of detection limits alone would hide the development problem. A2 has an exceptionally low miR-106b detection limit, but the full sample-to-answer time is not stated. A6 uses a familiar QCM immunoassay format for prostate-specific antigen, but numerical assay time is absent. A1 is fast and sensitive, but its lateral-field resonator creates a hardware-transfer question. The BREC matrix therefore places each sensor in a lane that corresponds to its first practical barrier.

The lane assignments in Table 3 answer the research question more directly than a scalar rank. A11, A3, and A8 are concordant because their targets are medically interpretable, their platforms are familiar, their recognition strategies are plausible, and their timing is compatible with near-patient use. A1 and A2 remain strong but require different next experiments: A1 needs hardware-transfer evidence, whereas A2 needs a complete molecular workflow. A9 and A10 are not failed sensors; their best validation path is chemical-recognition testing rather than bedside diagnosis.

The platform views in Figure 5 connect the readiness lanes to laboratory implementation. They show why a recognizable QCM-like hardware chain can reduce transfer uncertainty, whereas specialized or hybrid devices require more operational documentation before their analytical advantage can be judged against instrument burden.

The hardware panels support the distinction between analytical strength and deployability. A sensor that uses a recognizable chip holder, controller, liquid-contact path, and response display can move more directly into repeatability and matrix testing. Specialized resonators may still be superior for a given analyte, but they need an explicit transfer plan before they can be placed in the clinical-concordant lane.

Table 3: BREC readiness lanes.

ID	Target analyte	Readiness lane	First bottleneck	Immediate validation action
A11	K562 cells associated with chronic myeloid leukemia	Clinical-concordant candidate	Matrix and cell-line specificity remain to be proven.	Test patient-like blood matrices, non-K562 cell controls, chip-to-chip precision, and storage stability.
A3	*Staphylococcus aureus*	Clinical-concordant candidate	Strain breadth and matrix selectivity need confirmation.	Challenge the immunosensor with clinical isolates, commensal bacteria, and realistic sample pretreatment.
A8	Procalcitonin	Clinical-concordant candidate	Calibration must be tied to clinically relevant decision intervals.	Perform serum or plasma calibration, imprecision testing, interference assessment, and comparator-method checks.
A1	Heat shock proteins from myeloma cells	Hardware-specific high performer	Fast, sensitive readout is tied to a less standardized lateral-field platform.	Compare the lateral-field format with a transferable cartridge or QCM-compatible implementation.
A2	miR-106b from cancer cells	Molecular-sensitivity high performer	Total sample-to-answer time and matrix handling are not explicit.	Define extraction, hybridization, washing, and readout time in a complete protocol.
A12	Lactoferrin	Protocol-completion target	Analytical range is stated, but timing and matrix context are incomplete.	Document total assay time, specimen matrix, cross-reactivity, and calibration precision across the stated range.
A7	Prostate-specific antigen	Hybrid-instrument verification target	QCM-D/SERS complexity must justify its diagnostic value.	Demonstrate whether Raman information improves discrimination beyond QCM response alone.
A5	N^6-methyladenine	Protocol-compression target	Three-hour operation and receptor handling limit near-patient use.	Shorten recognition and readout steps while preserving methylation selectivity.
A6	Prostate-specific antigen	Documentation-completion target	Clinically familiar QCM immunoassay lacks numerical assay time.	Add a timed protocol, matrix tests, dynamic range, and decision-threshold calibration.
A10	Biotin methyl ester and biotinyl moieties	Chemical-recognition target	Strong synthetic recognition is not directly linked to bedside diagnosis.	Redirect validation toward chemical exposure, process monitoring, or affinity-selective quality control.
A9	*N*-nitroso-*l*-proline	Chemical-recognition target	Medical point-of-care anchoring is weaker than analytical chemistry relevance.	Compare against toxicology, food-safety, nitrosamine-monitoring, or process-control requirements.
A4	Antibodies against SARS-CoV-2	Documentation-repair target	Detection and assay duration are too approximate for development planning.	Define limit of detection, range, timing, matrix, specificity panel, replicates, and wafer reproducibility.

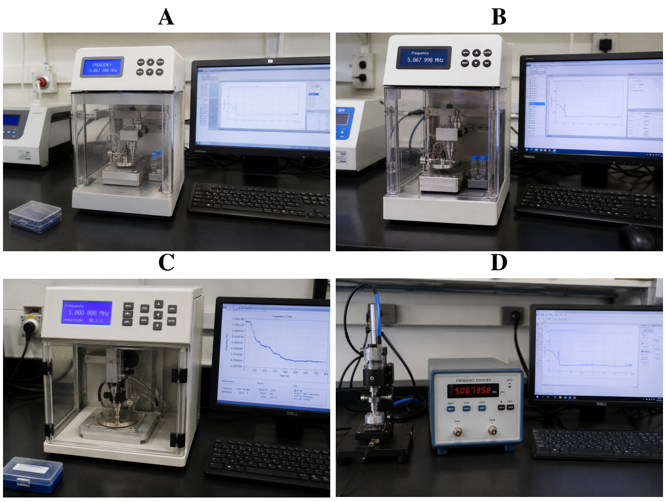

Figure 5: QCM handling and readout.

3.2. Clinical-concordant candidates

Three sensors formed the clinical-concordant lane. A11, the K562 cell aptasensor, is notable because cell-level detection is a demanding target class. The 263-cell detection limit and approximate 40-min assay time create a plausible measurement window for hematological use. Its next challenge is not basic proof of aptameric QCM response; it is matrix verification, specificity against non-target cells, and reproducibility of the aptamer-modified chip.

A3, the *S. aureus* QCM immunosensor, combines a low microbial burden with a 30-min assay window. This pairing is valuable because pathogen detection loses clinical utility when reporting time becomes too long. The lane assignment nevertheless remains cautious. A microbial QCM immunosensor must still address strain diversity, nonspecific adsorption, specimen pretreatment, and the difference between buffer-spiked performance and clinical-specimen behavior.

A8, the procalcitonin QCM biosensor, also belongs in the clinical-concordant lane because it joins a medically interpretable inflammatory marker with a sub-hour workflow and a familiar mass-sensitive platform. Its next experiment differs from A3 and A11. For procalcitonin, calibration near clinical decision intervals, imprecision at relevant concentrations, serum or plasma interference, and comparison with established immunoassays are more important than further sensitivity claims.

The preparation and platform-harmonization view in Figure 6 illustrates the operational conditions that the clinical-concordant candidates must satisfy next. Weighing, standards, chip handling, and instrument arrays form the traceability chain through which a promising resonator response becomes a reproducible analytical procedure.

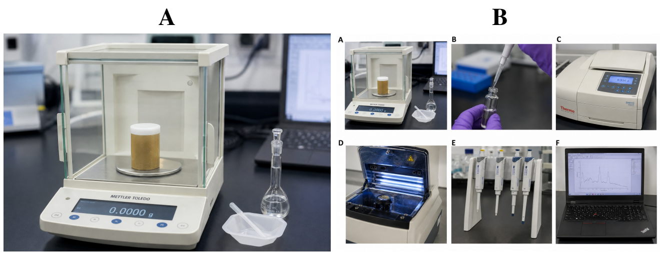

Figure 6: Preparation and platform harmonization.

The paired views define the operational bridge between prototype sensitivity and analytical validation. A candidate in the strongest BREC lane should now be tested through controlled preparation, replicate chips, lot-to-lot receptor deposition, and instrument-to-instrument reproducibility. Without that bridge, a fast and sensitive piezoelectric assay remains a bench demonstration rather than a diagnostic measurement system.

3.3. Conditional sensors and bottleneck-specific actions

A1 and A2 show why BREC separates signal quality from translation bottleneck. The heat shock protein assay has excellent sensitivity and the fastest stated time, but the lateral-field resonator creates a hardware-transfer question. A platform-comparison experiment would be more useful than another sensitivity experiment. By contrast, the miR-106b assay has a very low molecular detection limit and a broad range, but the missing sample-to-answer time prevents placement in the clinical-concordant lane. Its immediate need is a complete molecular workflow that covers extraction, hybridization, washing, readout, and matrix tolerance.

The two prostate-specific antigen sensors show different bottlenecks for the same clinical marker. A6 uses a familiar QCM immunoassay format and a low concentration limit, but numerical assay time is absent. A7 uses an aptameric QCM-D/SERS configuration with rapid readout described in minutes, yet the hybrid instrument must prove that Raman information changes diagnostic interpretation. The question is therefore not which PSA assay has the lower detection limit. The relevant issue is whether the low-limit QCM assay can supply missing workflow detail and whether the hybrid assay can justify added hardware.

A5 and A12 are protocol-completion cases. N^6-methyladenine detection has strong molecular sensitivity, but a three-hour assay is difficult to reconcile with near-patient use unless the clinical decision tolerates delayed reporting. Lactoferrin detection has an aptameric QCM format and a stated range, but absent timing and matrix context prevent stronger development placement. Both sensors need detailed protocol documentation and specimen-specific interference studies before diagnostic readiness can be claimed.

A9 and A10 demonstrate that target context changes the proper validation path. Molecularly imprinted polymer recognition is valuable in analytical chemistry, especially when synthetic receptors improve robustness and storage. Their lower medical-diagnostic placement in this study reflects target-context mismatch, not failure of the chemistry. Food safety, chemical exposure, process monitoring, or affinity-selective quality control would provide more suitable decision requirements for these two sensors.

A4 is the clearest documentation-repair case. It targets SARS-CoV-2 antibodies, a medically relevant class, yet its detection statement is approximate and its assay duration spans minutes to hours. That breadth is too large for near-patient planning. Exact analytical limits, working range, time-to-result, sample matrix, specificity panel, replicate structure, and wafer-to-wafer variability are required before comparison with better documented architectures.

The quality-control view in Figure 7 reinforces the interpretation of these conditional sensors. Sensor development depends on instrument stability, sample positioning, chip conditioning, and response documentation. BREC assigns penalties to missing operational descriptions because those omissions directly obstruct replication and validation, not because the sensor concept lacks scientific merit.

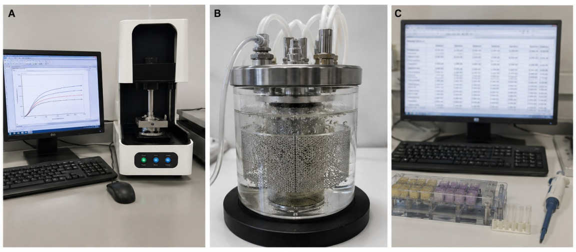

Figure 7: Frequency-assay quality control.

The quality-control image gives practical meaning to the documentation gate. A laboratory attempting to reproduce a piezoelectric assay must know whether chip conditioning, washing, stabilization, frequency-drift correction, temperature control, and endpoint selection were handled consistently. When these items are absent, the first bottleneck is documentation even if the target and sensitivity appear promising.

3.4. Action paths from the first bottleneck

The first action path for each non-concordant lane is summarized in Table 4. The table is not a speculative performance forecast; it identifies the most useful experiment or documentation item for each architecture. This shifts the analysis from ranking to development design: each sensor is linked to a concrete step that would make the next comparison fairer and more analytically meaningful.

The action matrix shows that additional work should be sensor-specific. A1 needs platform evidence more than a lower detection limit. A2 and A6 need timed protocols. A7 needs proof that the spectroscopic channel improves discrimination. A9 and A10 need non-bedside validation requirements. A3, A8, and A11 need matrix validation and precision testing rather than re-ranking. This specificity is the main practical output of BREC.

The assay-readout panels in Figure 8 connect the action matrix to documentation practice. Sample layouts, instrument screens, chip positions, and readout contexts are interpreted as traceability elements. Reproducible assay development depends on consistent physical arrangement and response logging, not only on a single attractive sensor image.

Figure 8: Assay readout documentation.

The readout panels reinforce a central methodological point: time-to-result and procedural completeness are assay properties. A sensor that does not state the full workflow duration cannot be evaluated fairly against a sensor that documents a 30- or 40-min procedure, even if the incomplete sensor has a lower detection limit.

4. Discussion

The BREC analysis changes the interpretation of piezoelectric diagnostic sensor comparison in three ways. First, it treats mixed analytical units as different measurement problems rather than values to be forced into a single ranking. This protects the analysis from assuming that the smallest numerical detection limit is automatically the strongest translational candidate. A picomolar nucleic-acid response, a CFU mL^{-1} microbial count, a cell-number threshold, and a ng L^{-1} inflammatory-marker result occupy different calibration spaces and must be interpreted in their biological decision contexts.

Second, the results show that translation is blocked by identifiable bottlenecks. The K562, *S. aureus*, and procalcitonin sensors are strongest because they are balanced across target relevance, platform familiarity, recognition plausibility, timing, and documentation. Their immediate need is formal validation. The heat shock protein and

Table 4: Bottleneck-specific action paths.

Bottleneck type	Affected sensors	Why it matters	Most useful next evidence
Hardware transferability	A1, partly A2 and A7	Specialized or hybrid platforms may be hard to standardize even when analytically strong.	Cartridge comparison, instrument-to-instrument reproducibility, and environmental stability testing.
Temporal uncertainty or delay	A2, A5, A6, A12, partly A4	Near-patient decisions require a defined sample-to-answer interval, not only a detection endpoint.	Timed workflow from specimen introduction to reportable result, including preparation and washing.
Hybrid-channel justification	A7	Dual-mode QCM-D/SERS readout increases information but also adds optical hardware and interpretation burden.	Ablation comparison showing whether the Raman channel improves discrimination or specificity.
Target-context mismatch	A9, A10	Chemically valuable targets may not be aligned with bedside medical decision making.	Toxicology, food-safety, chemical-exposure, or process-control validation requirements.
Documentation repair	A4	Approximate detection and broad timing prevent replication and fair comparison.	Complete analytical description with LOD, range, matrix, specificity, timing, replicate number, and wafer variability.
Clinical-concordance validation	A3, A8, A11	Strong sensors still require formal analytical validation before clinical claims.	Matrix interference, precision, stability, comparator methods, and clinically relevant specimen testing.

miR-106b sensors are analytically strong, but they do not require the same next experiment: one needs hardware-transfer evidence, while the other needs a complete molecular workflow.

Third, BREC separates analytical chemistry value from medical point-of-care alignment. Molecularly imprinted polymer sensors may be excellent candidates for chemical recognition, toxicology screening, or process monitoring, but the targets in this dataset are less directly connected to bedside diagnosis than K562 cells, procalcitonin, prostate-specific antigen, or *S. aureus*. The method therefore does not dismiss them as weak sensors; it places them under a more suitable development question.

The practical implication is that piezoelectric diagnostic studies should include a minimum operational evidence package. Limit of detection should be accompanied by dynamic range, specimen matrix, sample volume, total assay time, chip conditioning, receptor immobilization route, drift-stabilization procedure, nonspecific binding control, replicate number, chip-to-chip variation, interference testing, storage condition, and comparator method where applicable. These details are consistent with broader expectations for diagnostic validation, where analytical sensitivity must be integrated with reproducibility, bias control, and decision-relevant interpretation [23–25].

The final platform-check view in Figure 9 brings together controller hardware, sample organization, chip handling, and response monitoring. It supports the conclusion that near-patient readiness is an instrument-level property, not a sensitivity claim attached to an isolated receptor surface.

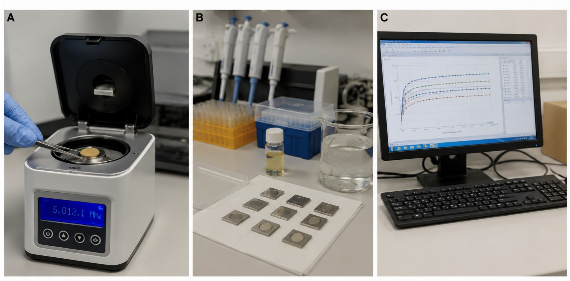

Figure 9: Platform readiness check.

The final check image emphasizes that a candidate assay must carry its receptor chemistry, surface preparation, resonator format, sample operation, readout trace, and validation evidence together. Weakness in any one component creates the first bottleneck and determines the next experiment. This interpretation is especially important for piezoelectric diagnostics because analytical sensitivity can improve while deployment readiness remains unchanged.

Several limitations should be recognized. The analysis uses tabulated sensor information rather than raw frequency traces, calibration replicates, patient-level measurements, or manufacturing files. BREC assignments therefore indicate development priorities rather than clinical accuracy. The gate language is transparent, but it still depends on expert judgment about what is sufficient for near-patient analytical planning. Food-safety or environmental-monitoring applications would use different timing and decision requirements. Cost-of-goods, regulatory feasibility, user-interface performance, shelf life, and maintenance burden are also outside the present analysis.

5. Conclusion

This study answered its research question by identifying which piezoelectric diagnostic sensors are concordant across near-patient analytical requirements and by specifying the first bottleneck for sensors that are not yet concordant. The strongest candidates are the QCM aptasensor for K562 cells, the QCM immunosensor for *Staphylococcus aureus*, and the QCM procalcitonin biosensor. They combine medically interpretable targets, plausible receptor chemistry, transferable resonator formats, usable timing, and enough procedural detail to justify matrix validation and precision testing. Heat shock protein detection and miR-106b detection remain analytically strong but are limited by different barriers: the first needs hardware-transfer evidence, whereas the second needs a complete sample-to-answer workflow. Prostate-specific antigen, lactoferrin, and N^6-methyladenine sensors require timed protocols, time compression, specimen-context testing, or proof that hybrid readout improves diagnostic discrimination. The molecularly imprinted polymer sensors should be advanced through chemical-recognition, toxicology, food-safety, or process-control validation rather than bedside diagnostic claims. The SARS-CoV-2 antibody wafer sensor requires exact analytical limits, working range, timing, matrix, specificity panel, replicate structure, and wafer-to-wafer variation before reliable comparison. The central conclusion is therefore direct: piezoelectric diagnostic translation is governed by the first unresolved bottleneck, not by detection limit alone. BREC provides a sensor-specific decision method for choosing validation, platform transfer, workflow completion, documentation repair, or target-context redirection.

References

[1] Sauerbrey, G. (1959). Verwendung von Schwingquarzen zur Wägung dünner Schichten und zur Mikrowägung. Zeitschrift für physik, 155(2), 206-222.

[2] Kanazawa, K. K., & Gordon, J. G. (1985). Frequency of a quartz microbalance in contact with liquid. Analytical Chemistry, 57(8), 1770-1771.

[3] Rodahl, M., Höök, F., Krozer, A., Brzezinski, P., & Kasemo, B. (1995). Quartz crystal microbalance setup for frequency and Q-factor measurements in gaseous and liquid environments. Review of Scientific Instruments, 66(7), 3924-3930.

[4] Marx, K. A. (2003). Quartz crystal microbalance: a useful tool for studying thin polymer films and complex biomolecular systems at the solution-surface interface. Biomacromolecules, 4(5), 1099-1120.

[5] Janshoff, A., Galla, H. J., & Steinem, C. (2000). Piezoelectric mass-

sensing devices as biosensors—an alternative to optical biosensors?. Angewandte Chemie International Edition, 39(22), 4004-4032.

[6] Cooper, M. A., & Singleton, V. T. (2007). A survey of the 2001 to 2005 quartz crystal microbalance biosensor literature: applications of acoustic physics to the analysis of biomolecular interactions. Journal of Molecular Recognition: An Interdisciplinary Journal, 20(3), 154-184.

[7] Länge, K., Rapp, B. E., & Rapp, M. (2008). Surface acoustic wave biosensors: a review. Analytical and bioanalytical chemistry, 391(5), 1509-1519.

[8] Arlett, J. L., Myers, E. B., & Roukes, M. L. (2011). Comparative advantages of mechanical biosensors. Nature nanotechnology, 6(4), 203-215.

[9] Lim, H. J., Saha, T., Tey, B. T., Tan, W. S., & Ooi, C. W. (2020). Quartz crystal microbalance-based biosensors as rapid diagnostic devices for infectious diseases. Biosensors and Bioelectronics, 168, 112513.

[10] Afzal, A., Mujahid, A., Schirhagl, R., Bajwa, S. Z., Latif, U., & Feroz, S. (2017). Gravimetric viral diagnostics: QCM based biosensors for early detection of viruses. Chemosensors, 5(1), 7.

[11] Ellington, A. D., & Szostak, J. W. (1990). In vitro selection of RNA molecules that bind specific ligands. nature, 346(6287), 818-822.

[12] Tuerk, C., & Gold, L. (1990). Systematic evolution of ligands by exponential enrichment: RNA ligands to bacteriophage T4 DNA polymerase. science, 249(4968), 505-510.

[13] Stoltenburg, R., Reinemann, C., & Strehlitz, B. (2007). SELEX—A (r) evolutionary method to generate high-affinity nucleic acid ligands. Biomolecular engineering, 24(4), 381-403.

[14] Whitcombe, M. J., Kirsch, N., & Nicholls, I. A. (2014). Molecular imprinting science and technology: a survey of the literature for the years 2004–2011. Journal of Molecular Recognition, 27(6), 297-401.

[15] Haupt, K., & Mosbach, K. (2000). Molecularly imprinted polymers and their use in biomimetic sensors. Chemical reviews, 100(7), 2495-2504.

[16] Nie, S., & Emory, S. R. (1997). Probing single molecules and single nanoparticles by surface-enhanced Raman scattering. science, 275(5303), 1102-1106.

[17] Drain, P. K., Hyle, E. P., Noubary, F., Freedberg, K. A., Wilson, D., Bishai, W. R., ... & Bassett, I. V. (2014). Diagnostic point-of-care tests in resource-limited settings. The Lancet infectious diseases, 14(3), 239-249.

[18] Justino, C. I., Duarte, A. C., & Rocha-Santos, T. A. (2016). Critical overview on the application of sensors and biosensors for clinical analysis. TrAC Trends in Analytical Chemistry, 85, 36-60.

[19] Vashist, S. K. (2017). Point-of-care diagnostics: Recent advances and trends. Biosensors, 7(4), 62.

[20] Dincer, C., Bruch, R., Kling, A., Dittrich, P. S., & Urban, G. A. (2017). Multiplexed point-of-care testing–xPOCT. Trends in biotechnology, 35(8), 728-742.

[21] Land, K. J., Boeras, D. I., Chen, X. S., Ramsay, A. R., & Peeling, R. W. (2019). REASSURED diagnostics to inform disease control strategies, strengthen health systems and improve patient outcomes. Nature microbiology, 4(1), 46-54.

[22] Heidt, B., Siqueira, W. F., Eersels, K., Diliën, H., van Grinsven, B., Fujiwara, R. T., & Cleij, T. J. (2020). Point of care diagnostics in resource-limited settings: a review of the present and future of PoC in its most needed environment. Biosensors, 10(10), 133.

[23] Pierson-Perry, J. F., Vaks, J. E., Vore, T. E. K., Durham, A. P., Fischer, C., Gutenbrunner, C., ... & Middleberg, R. A. (2012). Evaluation of detection capability for clinical laboratory measurement procedures; approved guideline. Clinical Laboratory Standards Institute.

[24] Bossuyt, P. M., Reitsma, J. B., Bruns, D. E., Gatsonis, C. A., Glasziou, P. P., Irwig, L., ... & STARD Group. (2015). STARD 2015: an updated list of essential items for reporting diagnostic accuracy studies. Radiology, 277(3), 826-832.

[25] Cohen, J. F., Korevaar, D. A., Altman, D. G., Bruns, D. E., Gatsonis, C. A., Hooft, L., ... & Bossuyt, P. M. (2016). STARD 2015 guidelines for reporting diagnostic accuracy studies: explanation and elaboration. BMJ open, 6(11), e012799.

[26] Pohanka, M. (2025). Piezoelectric chemosensors and biosensors in medical diagnostics. Biosensors, 15(3), 197.